DRAFT VERSION FEBRUARY 19, 2021
Typeset using LATEX **twocolumn** style in AASTeX63

Wind mass-loss rates of stripped stars inferred from Cygnus X-1

COENRAAD J. NEIJSSEL,[1,2,3] SERENA VINCIGUERRA,[4,2,3,5] ALEJANDRO VIGNA-GÓMEZ,[6] RYOSUKE HIRAI,[2,3] JAMES C. A. MILLER-JONES,[7] ARASH BAHRAMIAN,[7] THOMAS J. MACCARONE,[8] AND ILYA MANDEL[2,3,1]

[1]*Birmingham Institute for Gravitational Wave Astronomy and School of Physics and Astronomy, University of Birmingham, Birmingham, B15 2TT, United Kingdom*
[2]*Monash Centre for Astrophysics, School of Physics and Astronomy, Monash University, Clayton, Victoria 3800, Australia*
[3]*The ARC Center of Excellence for Gravitational Wave Discovery – OzGrav*
[4]*Max Planck Institute for Gravitational Physics (Albert Einstein Institute), D-30167 Hannover, Germany*
[5]*Anton Pannekoek Institute for Astronomy, University of Amsterdam, Science Park 904, 1090GE Amsterdam, The Netherlands*
[6]*DARK, Niels Bohr Institute, University of Copenhagen, Blegdamsvej 17, 2100 Copenhagen, Denmark*
[7]*International Centre for Radio Astronomy Research – Curtin University, GPO Box U1987, Perth, WA 6845, Australia*
[8]*Department of Physics & Astronomy, Texas Tech University, Box 41051, Lubbock TX, 79409-1051, USA*

(Received February 19, 2021)

ABSTRACT

Recent observations of the high-mass X-ray binary Cygnus X-1 have shown that both the companion star (41 solar masses) and the black hole (21 solar masses) are more massive than previously estimated. Furthermore, the black hole appears to be nearly maximally spinning. Here we present a possible formation channel for the Cygnus X-1 system that matches the observed system properties. In this formation channel, we find that the orbital parameters of Cygnus X-1, combined with the observed metallicity of the companion, imply a significant reduction in mass loss through winds relative to commonly used prescriptions for stripped stars.

Keywords: Stellar mass black holes, High mass x-ray binary stars, Stellar winds

1. INTRODUCTION

Cygnus X-1 is a high-mass X-ray binary (HMXB) in the Cygnus OB3 association, which hosts a star in orbit with a black hole (BH) (e.g. Webster & Murdin 1972; Bolton 1972, 1975; Hutchings et al. 1973). The BH accretes matter from the stellar wind; this accretion powers X-ray radiation (e.g. Davidson & Ostriker 1973; van den Heuvel 1975; Conti 1978; Petterson 1978) and a jet (e.g. Bisiacchi et al. 1974; Marti et al. 1996; Stirling et al. 2001). Orosz et al. (2011) inferred the BH and stellar companion masses of Cygnus X-1 to be $14.8 \pm 1.0 M_\odot$ and $19.2 \pm 1.9 M_\odot$, respectively. Revised measurements of the distance to Cygnus X-1 (Miller-Jones et al. 2021) indicate that both objects are significantly more massive. The temperature and luminosity of the optical companion are estimated to be $T_{\rm eff} = 31.1 \pm 0.7$ kK and $\log(L/L_\odot) = 5.63 \pm 0.07$ with a mass of $M_{\rm opt} = 40.6^{+7.7}_{-7.1} M_\odot$, where we quote the median value and the 68 per cent confidence interval boundaries (Miller-Jones et al. 2021). The mass of the BH is estimated as $M_{\rm BH} = 21.2^{+2.2}_{-2.3} M_\odot$. The binary has an almost circular orbit with a semi-major axis $a = 0.244^{+0.012}_{-0.013}$ AU and eccentricity $e = 0.0189^{+0.0028}_{-0.0026}$ (Miller-Jones et al. 2021). The BH is inferred to be nearly maximally spinning with a dimensionless spin of at least 0.95 according to both disk continuum and reflection line fitting studies (Gou et al. 2011; Fabian et al. 2012; Miller-Jones et al. 2021; Zhao et al. 2021). Via optical spectroscopy, it has been found that the ratios of the surface abundances of both helium and iron to hydrogen are about twice the respective values for the Sun (Shimanskii et al. 2012). As we discuss below, these observations taken together present a challenge for models of massive stellar binary evolution.

In this paper we describe the constraints that these observations place on the Cygnus X-1 formation channel (Sec. 2). We explore how the helium main sequence (HeMS) phase of this channel provides a constraint on the wind mass-loss rates of massive stars (Sec. 3). We present the likely future of the system and its implications for gravitational-wave detections (Sec. 4). Finally we discuss some caveats and questions raised by the observations of Cygnus X-1 (Sec. 5).

cneijssel@star.sr.bham.ac.uk
ilya.mandel@monash.edu

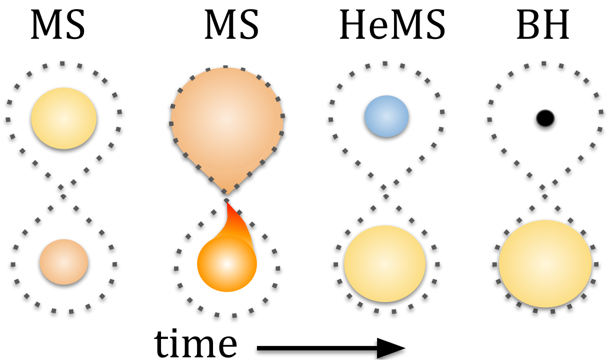

Figure 1. Assumed formation channel for Cygnus X-1. 1: Two stars (primary top, secondary bottom) are born in a binary. 2: The primary star is more massive and evolves faster, expands and starts stable mass transfer onto the secondary. 3: The primary is left as a hot stripped HeMS star with a companion which could have accreted a significant amount. 4: The primary star collapses and leaves behind a BH orbiting the secondary MS star.

2. CYGNUS X-1: OBSERVATIONS AND ASSUMED CHANNEL

We assume the following formation channel for Cygnus X-1 (see Fig.1 for illustration). Two stars are born in a binary. The more massive star (the primary) evolves more quickly and expands first. The companion (the secondary) is close enough for the late main sequence primary to commence mass transfer. The primary is stripped of its envelope, leaving an exposed helium core. The core continues nuclear fusion until it collapses and forms a BH in orbit with the still core-hydrogen-burning main sequence (MS) companion. In the sections below, we describe the observations and theoretical analyses that support this channel.

2.1. *Eccentricity, peculiar velocity and fallback*

The collapse of a star into a compact object can impart both a natal kick from an asymmetric explosion (see e.g. Fryer 2004 and references therein) and a kick from rapid symmetric mass loss to the system (Blaauw 1961). The low eccentricity of the Cygnus X-1 binary (Orosz et al. 2011; Miller-Jones et al. 2021) seems to disfavour a significant natal kick. However, tidal forces could have circularised the system since the collapse: for the inferred stellar and binary properties, the circularisation timescale for dynamical tides (applicable for radiative-envelope stars, Zahn 1977) is only $\sim 10^5$ years (estimated using equations (41) and (43) of Hurley et al. 2002).

On the other hand, the system's small peculiar velocity strongly indicates that the BH experienced nearly complete collapse with little mass ejection during its formation (Mirabel & Rodrigues 2003). The peculiar velocity is 10.7 ± 2.7 km s^{-1} relative to its host association (Rao et al. 2019), which limits the amount of instantaneous symmetric mass loss (Blaauw 1961; Nelemans et al. 1999; Wong et al. 2012) to $\lesssim 2 M_\odot$, unless the kick from symmetric mass ejection is fortuitously cancelled by an oppositely directed natal kick. Further indirect evidence for the low natal kick lies in the absence of Type C quasi periodic oscillations, which may indicate Lense-Thirring precession due to spin-orbital misalignment as a result of a natal kick (Stella & Vietri 1998) and are observed in most known black hole X-ray binaries (Ingram et al. 2016), the majority of which are believed to have received strong (~ 100 km s^{-1}) natal kicks (Atri et al. 2019). The low amount of ejected mass is also consistent with the current eccentricity in the absence of significant tidal circularisation, and suggests nearly complete fallback onto the black hole except for a small amount of neutrino mass loss (e.g. Nadezhin 1980; Lovegrove & Woosley 2013; Fernández et al. 2018). Nearly complete collapse matches the theoretical models simulating the fall-back onto black holes of similar masses (Fryer et al. 2012) and observational evidence for massive stars disappearing without supernovae (Adams et al. 2017).

2.2. *Black-hole progenitor mass*

The Eddington limit on the mass accretion rate for a BH of this mass is $\lesssim 2 \times 10^{-7} M_\odot$ yr^{-1}. Under the assumption of Eddington-limited accretion (but see, e.g., Fragos & McClintock 2015; Eldridge et al. 2017; van Son et al. 2020, who relax this assumption), only a negligible amount of mass could have been accreted onto the BH since it formed (King & Kolb 1999). The companion lifetime sets the accretion duration to no more than a few Myr, meaning that at most $\lesssim$ few $\times 10^{-1} M_\odot$ could have been accreted. Assuming that the jet turned on promptly after the formation of the black hole, the few$\times 10^4$ yr estimate of the age of the jet (Russell et al. 2007) places an even stronger constraint on the amount of accreted mass, $\lesssim 10^{-2} M_\odot$ (see also Sell et al. 2015, who consider other models for the nebula origin but reach similar conclusions about its age). Therefore, the current black hole mass $M_{\rm BH} = 21.2^{+2.2}_{-2.3} M_\odot$ is a good estimate for the progenitor mass just before the collapse.

2.3. *Black hole spin & progenitor spin*

The BH has a dimensionless spin χ close to unity, $\chi \geq 0.95$ (Gou et al. 2011; Fabian et al. 2012; Miller-Jones et al. 2021), although spin measurements may have large systematic errors because of modelling assumptions (Miller & Miller 2015; Kawano et al. 2017; Zhao et al. 2021). A spin close to unity, coupled with negligible mass loss during collapse, suggests that if the pre-collapse progenitor had excess angular momentum, $\chi > 1$, it must have been carried away by a small amount of mass with high specific angular momentum (cf. Janka 2013, 2017; Batta & Ramirez-Ruiz 2019; Murguia-Berthier et al. 2020).

The rotational angular momentum of the BH was either present in the progenitor, or was gained during or after its collapse. Here we briefly summarise why we assume that the angular momentum comes from the progenitor and why this implies that the progenitor must have been stripped early in its evolution (see Mandel & Fragos 2020 for a longer discussion).

A BH needs to roughly double its mass through accretion in order to go from zero to maximal spin (Bardeen et al. 1973; Thorne 1974). This is not possible for Cygnus X-1 under the assumption of Eddington-limited accretion. The spin could have been acquired during the collapse, e.g., if the companion torques some of the ejecta which then fall back onto the BH (Batta et al. 2017; Schrøder et al. 2018), but this requires some fine-tuning: for example, the ejecta must have sufficient velocities to be torqued by the companion, but without a significant tail of escaping ejecta to match formation through nearly complete fallback as discussed above. Therefore we assume that the angular momentum was present in the progenitor at the moment of the collapse.

Observations suggest that stars might be born as rapid rotators (Fukuda 1982; Rosen et al. 2012; Ramírez-Agudelo et al. 2013, 2015), although these observations could be affected by binary interactions (Langer et al. 2008; de Mink et al. 2013). Even if stars are born as rapid rotators, they spin down through wind-driven mass loss and are unlikely to retain enough angular momentum to form rapidly spinning BHs.

The black hole's dimensionless spin is determined by the ratio of its total angular momentum to the square of its mass. At lowest order, it is therefore insensitive to the redistribution of angular momentum through the progenitor star. However, if the bulk of the angular momentum moves into the envelope as the star expands, and the envelope is subsequently removed by winds or mass transfer, the remaining core is likely left with too little angular momentum to produce a rapidly spinning BH (Petrovic et al. 2005; Belczynski et al. 2017; Fuller & Ma 2019; Bavera et al. 2020; Mandel & Fragos 2020). On the other hand, the core could retain sufficient angular momentum to form a rapidly spinning BH if there is a large amount of differential rotation between the layers of the star (Hirschi et al. 2005). Therefore, the efficiency of angular momentum transport in the star plays a key role, yet both the mechanism and degree of core-envelope coupling remain uncertain. Theory (Tayler 1973; Spruit 2002; Fuller et al. 2019; Takahashi & Langer 2020) and observations, such as rotation rates of low-mass giant stars (Cantiello et al. 2014), suggest that there may be efficient angular momentum transport and the envelope is coupled to the core. If so, the observed rapid spin of the Cygnus X-1 black hole in a close binary, in which the progenitor must have lost its envelope, appears to require pre-collapse interaction with the companion to spin up the stellar core.

Tidal locking of the period of the stellar rotation to the period of the binary provides the most likely mechanism for producing a rapidly rotating BH progenitor (Izzard et al. 2004; Kushnir et al. 2016; Zaldarriaga et al. 2018; Belczynski et al. 2017; Bavera et al. 2020). Chemically homogeneous evolution could yield rapidly rotating black holes (Mandel & de Mink 2016; Marchant et al. 2016), but is not expected to operate at such high metallicities and is not consistent with the observed expansion of the companion.

Instead, the following evolutionary sequence, proposed by Valsecchi et al. (2010) for M33 X-7, a similar high-mass X-ray binary with a rapidly spinning BH, and investigated in detail by Qin et al. (2019), appears to be the most likely formation mechanism for Cygnus X-1. The binary starts out with a period somewhat shorter than the current observed one. The more massive primary – the BH progenitor – commences mass transfer while still on the main sequence. This mass transfer, is likely to be largely non-conservative if limited by the spin-up of the accretor (Qin et al. 2019); this is favoured both by the observed evolutionary state of the secondary (conservative mass transfer would imply an initially lower-mass primary, and hence an older binary, placing an upper limit on the BH progenitor mass that would make it unlikely to form such a massive BH) and the observed period. The mass transfer removes the donor's envelope, preventing subsequent re-expansion and angular momentum loss. Meanwhile, the core remains tidally locked on the MS. After hydrogen is exhausted in the core at the end of the MS, the star contracts into a rapidly spinning HeMS star. While this HeMS star is no longer tidally locked, it can still collapse into a rapidly spinning BH. Qin et al. (2019) find that the efficiency of angular momentum transport does not play a significant role for the evolution of the black hole progenitor during the main sequence, where tidal locking keeps its core rapidly spinning, but could be a key factor in determining the ultimate black hole spin through its impact on the angular momentum lost through winds in later evolutionary stages. The Qin et al. (2019) models successfully reproduce systems with the orbital parameters of Cygnus X-1. In fact, the match appreciably improves with the upward revision in the BH and optical companion masses, as the observed masses in the bottom left panel of figure 3 of Qin et al. (2019) shift toward the locus of their model evolutionary trajectories (though their evolutionary trajectories are only shown for an initial mass ratio of 0.4, while the latest observations support more comparable masses). Given the number of uncertainties relating to this first mass transfer episode, in what follows we focus on the subsequent evolution of the binary under the assumption of this formation channel for Cygnus X-1.

2.4. *Companion mass & abundance*

We compared the observed mass, luminosity and temperature of the optical companion against analytic fits to stellar tracks of Hurley et al. (2000) as implemented in the COMPAS rapid population synthesis code (Stevenson et al. 2017; Vigna-Gómez et al. 2018). The observations are consistent with a MS star that is about 70 to 80 per cent through its core hydrogen burning phase, ignoring the impact of rotation.

These stellar tracks are for stars with regular hydrogen-rich atmospheres. Using them ignores the possible impact of non-standard surface abundances, and so corresponds to the assumption that only a thin surface layer has a significant over-abundance of helium, rather than a uniform distribution of enriched material throughout the star. Stars in later stages of the MS with the relevant mass and metallicity should have at most a very thin convective layer at the surface (e.g., Maeder et al. 2008; Kippenhahn et al. 2012). Therefore, mixing is expected to be relatively inefficient: in the absence of large-scale convection, the Rayleigh-Taylor instability is likely to be suppressed by temperature inversion in the accreted material (Kippenhahn et al. 1980; Braun & Langer 1995). The resulting thermohaline mixing will mix the helium-rich material through the companion only on timescales longer than the expected few$\times 10^4$ years since the formation of the BH if the bulk of the enriched material was accreted at or shortly before the BH formation.

The evolutionary channel shown in figure 1 assumes that the optical companion has not overflowed its Roche lobe. While previous studies explored this possibility, perhaps with intermittent Roche lobe overflow followed by longer periods when the binary is detached as in the present state, these models were typically based on assumptions that the companion is less massive than the BH (Podsiadlowski et al. 2003), which is inconsistent with present observations. Indeed, if we assume that mass transfer onto a black hole is almost entirely non-conservative because of the Eddington limit, the binary's semi-major axis a evolves as

$$\frac{\dot{a}}{a} = -2\frac{\dot{M}_{\rm opt}}{M_{\rm opt}}\left[1-\left(\gamma+\frac{1}{2}\right)\frac{M_{\rm opt}}{M_{\rm opt}+M_{\rm BH}}\right], \qquad (2.1)$$

where γ is the specific angular momentum of the ejected material in units of the binary's specific orbital angular momentum $J/(M_{\rm opt}+M_{\rm BH})$. The binary can widen as a result of such mass transfer only if $\gamma \lesssim 1$ for the observed component masses. However, in the common assumption of isotropic re-emission from the accretor, $\gamma = M_{\rm opt}/M_{\rm BH} \approx 2$. The ejected material would have to carry much lower specific angular momentum in order for the binary to be able to detach once Roche lobe overflow from the companion commences, which seems unlikely, lending support to our proposed channel.

The estimated mass and lifetime of the companion already enable us to roughly infer the initial mass of the BH progenitor. We assume that both stars are born and start fusion at the same time and use a fit (Farr & Mandel 2018) to the Brott et al. (2011); Köhler et al. (2015) stellar models for the MS lifetime of non-rotating massive stars. For this simple estimate, we ignore the impact of binary interactions, consistent with the assumption of largely non-conservative mass transfer. The BH progenitor should have had an initial mass of $\sim 55 - 75 M_\odot$ in order to complete its evolution while leaving behind a MS companion of mass $M_{\rm opt}$ at $\sim 70\% - 80\%$ of its MS lifetime.

The surface abundances of the companion are non-standard for massive MS stars and a challenge to explain even in the context of binary interaction. We discuss the abundances in more detail in Section 5. Here, we focus on the iron abundance, as this is key to the analysis of line-driven winds in the following section. Shimanskii et al. (2012) find that the iron abundance of the companion is 2.2 times the solar iron abundance, although precise measurements are challenging due to the complexity of the system. Assuming $Z_\odot = 0.014$ for solar metallicity (Asplund et al. 2009), this corresponds to an effective metallicity of $Z \approx 0.03$. On the other hand, Daflon et al. (2001) find a slightly sub-solar iron abundance of $\log\epsilon({\rm Fe}) = 7.33 \pm 0.12$ in HD 227460, which is a B0.5V star in the same Cygnus OB3 association as Cygnus X-1. This could indicate that $Z \approx 0.01$ is a better estimate of the initial iron abundance, and the iron abundance of the companion in Cygnus X-1 has been enhanced during the collapse of the primary to a BH. Therefore, we explore an initial metallicity range $0.01 \leq Z \leq 0.03$ in the following section.

3. CYGNUS X-1: MAXIMUM WIND MASS-LOSS RATE

Hereafter we assume that, after the mass transfer episode induced by the BH progenitor, the primary is left with no hydrogen layer on top of the He core. This assumption is consistent with the channel proposed by Qin et al. (2019), in which the rapidly spinning BH is ultimately formed through the collapse of a Wolf-Rayet star (see however discussion in Section 5).

In order for Cygnus X-1 to form through the channel depicted in Fig. 1, two things must be true. Firstly, the HeMS star must be born with sufficient mass to give rise to the observed BH mass even after losing mass through Wolf-Rayet winds during the HeMS. However, at a given metallicity, there is a maximum to the He core mass that can be formed at the end of the MS: as more massive stars have higher wind mass loss rates, terminal-age MS He core masses asymptotically approach a maximum as a function of zero-age MS. This maximum He core mass is plotted in figure 2. Because the BH progenitor is stripped of its hydrogen envelope at the end of the MS for the binary evolutionary channel we assume, we can directly constrain the amount of mass

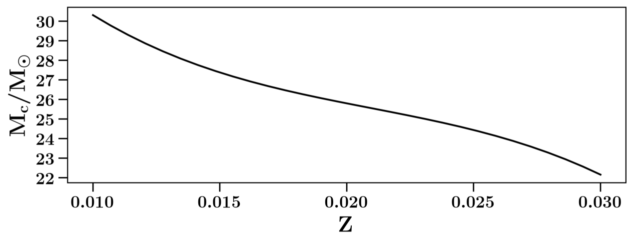

Figure 2. Maximum helium core mass at terminal-age MS as a function of metallicity, maximized over zero-age MS masses, based on the stellar tracks of Hurley et al. (2000) as implemented in COMPAS (Stevenson et al. 2017; Vigna-Gómez et al. 2018).

loss during the HeMS phase. The Wolf-Rayet winds must then not remove more than the difference between this maximum mass and the final BH mass. We refer to this as the "$M_{\rm HeMS} \leq M_{\rm HeMS,max}$" condition.

The maximum He core mass plotted in figure 2 is very sensitive to the MS wind prescriptions (see discussion in Renzo et al. 2017; Neijssel et al. 2019; Miller-Jones et al. 2021). The analysis of the remnant mass from massive single stars is particularly sensitive to luminous blue variable winds (Belczynski et al. 2010; Miller-Jones et al. 2021), which can remove the hydrogen envelope of the star and hasten the onset of the Wolf-Rayet phase (Conti 1975); therefore, increasing the potential remnant mass can be achieved by decreasing either luminous blue variable winds or Wolf-Rayet winds. The plot in figure 2 assumes the default COMPAS luminous blue variable mass loss rate of $1.5 \times 10^{-4} \rm M_\odot\ yr^{-1}$ (Belczynski et al. 2010) for stars approaching the Humphreys-Davidson limit (Humphreys & Davidson 1994). The convective overshooting parameter employed in stellar evolution calculations is another source of uncertainty, with greater overshooting leading to larger cores (Brott et al. 2011). To explore the impact of convective overshooting, we simulated the He core mass at terminal-age MS for stars with different metallicities starting from a zero-age MS mass of 150 $\rm M_\odot$ using the stellar evolution code MESA (v12115, Paxton et al. 2011). We find that varying the overshooting parameter by an order of magnitude between $f = 0.02$ and $f = 0.2$ (Qin et al. 2019 used $f = 0.11$) with the step overshoot scheme changes the He core mass at terminal-age MS by between 1% and 13% for the range of metallicities in figure 2. Finally, the COMPAS single stellar evolution models are based on the fitting formulae of Hurley et al. (2000) to the evolutionary tracks of Pols et al. (1998) which involve extrapolations to higher masses than those covered by the initial range of models, and may under-estimate the He core masses of massive stars. We therefore use the following additional constraint, which bypasses these sources of uncertainty in the maximum He core mass.

In our assumed channel the secondary MS companion must not overflow its Roche lobe onto the HeMS primary. We write this constraint as (Eggleton 1983)

$$R_2(t) \leq a(t)\frac{0.49q^{2/3}(t)}{0.6q^{2/3}(t) + \ln(1+q^{1/3}(t))}, \tag{3.1}$$

where $m_2(t)$ and $R_2(t)$ are the mass and radius of the companion as a function of time, $m_1(t)$ the mass of the BH or its progenitor, $q(t) = \frac{m_2(t)}{m_1(t)}$, is the mass ratio, and $a(t)$ the orbital separation of the binary.

The orbital separation widens due to wind mass loss. In the limit of fast, non-interacting winds, the widening is described by

$$\frac{\dot{a}}{a} = -\frac{\dot{M}_{\rm tot}}{M_{\rm tot}}, \tag{3.2}$$

where $M_{\rm tot} = m_1 + m_2$ is the total mass of the system. Because winds widen the binary and remove mass from the HeMS primary faster than from its MS companion, they increase the size of the secondary's Roche lobe over time. Thus, even though the secondary is not overflowing its Roche lobe now, it may have done so in the past if the mass-loss rate was high. If we evolve the system back in time, the requirement that the secondary never overflows its Roche lobe imposes an alternative upper limit (Axelsson et al. 2011) on the maximum Wolf-Rayet wind mass-loss rate. We refer to this as the *"no Roche-lobe overflow (RLOF)"* condition. Although the non-interacting wind assumption, describing the widening of the binary (Equation 3.2), may be an over-simplification for such short-period systems (MacLeod & Loeb 2020), it allows us to conservatively estimate the constraints imposed by the existence of Cygnus X-1 and presented below.

We parametrise the mass-loss rate through Wolf-Rayet winds, modelled with the prescription proposed by Belczynski et al. (2010) and based on (Hamann et al. 1995; Hamann & Koesterke 1998; Belczynski et al. 2010), with a multiplicative parameter $f_{\rm WR}$, following Barrett et al. (2018) (see Appendix A for a definition and discussion). We constrain the allowed parameter space of the wind strength by rewinding the evolution of the binary from the current state. Because the BH formed recently in our model, we set the luminosity and temperature of the MS companion at the end of the HeMS phase of the primary equal to the current inferred luminosity and temperature of the observed MS secondary. The mass and age of the secondary inferred from temperature and luminosity vary slightly for different metallicities. As we argued earlier, the BH is expected to lose negligible mass during collapse, so we set the mass of the HeMS primary at the end of that phase equal to the inferred BH mass. We assume that the secondary was 99.7% Roche-lobe filling at the end of the primary's HeMS phase (Miller-Jones et al. 2021)[1].

The reverse evolution of the MS and HeMS stars is followed using the analytic fits to the stellar tracks of Pols et al. (1998) as presented in Hurley et al. (2000). The winds of the MS star are given by Vink et al. (2001). The HeMS winds are parametrised with the multiplicative factor $f_{\rm WR}$ as described above and in Appendix A. The orbital response to mass loss is given by Eq. (3.2). We go back in the evolution for a HeMS lifetime (note that the HeMS lifetime depends on how massive the HeMS star initially was, which depends on the wind strength we assume) and check that the $M_{\rm HeMS} \leq M_{\rm HeMS,max}$ condition is satisfied at the start of the HeMS phase and the *no RLOF* condition is satisfied throughout this phase.

Figure 3 shows the upper limits on the wind strength, parametrized as $f_{\rm WR}$, imposed by these two conditions as a function of metallicity. Both conditions show that the wind strength has to be reduced from the nominal value $f_{\rm WR} = 1$ throughout the range of metallicities we have explored. The strongest constraint is placed by the $M_{\rm HeMS} \leq M_{\rm HeMS,max}$ condition, which is subject to uncertainties in the MS wind strengths, overshooting, and the single stellar evolution fits of Hurley et al. (2000). This yields an upper limit $f_{\rm WR} \lesssim 0.4$ at $Z = 0.01$ and $\lesssim 0.05$ at $Z = 0.03$. However, even if we lift this constraint, the *no RLOF* condition still places a strong constraint on the allowed mass loss rate: $f_{\rm WR} \lesssim 0.45$ at $Z = 0.01$ and $\lesssim 0.15$ at $Z = 0.03$. We also explore the impact of BH mass and Roche-lobe filling factor measurement uncertainties and find that the constraints on $f_{\rm WR}$ change by $\lesssim 0.1$ over the range consistent with observations (Miller-Jones et al. 2021).

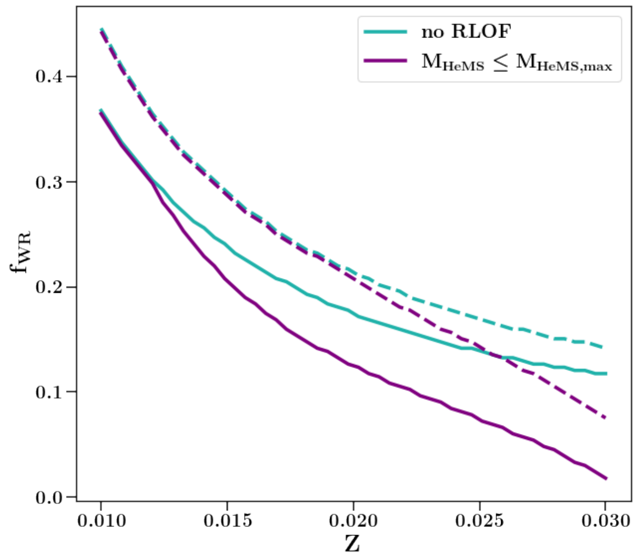

Figure 3. Upper limits on the parametrised Wolf-Rayet wind mass loss rate from HeMS stars. The $M_{\rm HeMS} \leq M_{\rm HeMS,max}$ (purple) and *no RLOF* (teal) conditions only allow $f_{\rm WR}$ values below the curves at metallicity Z. The dashed curves correspond to assuming $M_{\rm BH} = 19.2 M_\odot$ and the current companion Roche-filling factor of 0.990 rather than the default values of $21.2 M_\odot$ and 0.997 (solid curves), and indicate the impact of observational uncertainty.

4. CYGNUS X-1: FUTURE EVOLUTION

The revised mass of the companion star in Cygnus X-1 makes it a potential candidate for a future BH and raises the intriguing prospect that this system could form a merging binary BH, connecting HMXBs with gravitational-wave sources. We model the future evolution of the system and find that it is unlikely to form a merging binary BH.

Belczynski et al. (2011) used earlier, lower estimates of the mass of the BH and companion in Cygnus X-1 in order to analyse the future evolution of this system. They predicted that imminent mass transfer from the nearly Roche-lobe filling companion will significantly reduce the companion mass, leaving behind a core that could only form a neutron star, not a BH. They further estimated that the natal kick has a 30% probability of unbinding the binary, and there was only a $\sim 1\%$ probability that the ensuing neutron star – black hole binary would merge within 14 Gyr through gravitational-wave emission.

Here we update their predictions based on revised observations, using the COMPAS population synthesis code (Stevenson et al. 2017; Vigna-Gómez et al. 2018) for binary evolution calculations. We estimate the initial masses and orbital separation as in Section 3. We assume a Roche lobe filling factor of 0.997 and a metallicity of $Z = 0.02$. The median values for the BH mass and the luminosity and temperature of the MS companion from Miller-Jones et al. (2021) then yield $M_{\rm BH} = 21.2 M_\odot$, $M_{\rm opt} = 38.9 M_\odot$, $a = 51.3 R_\odot$, and $\tau_{\rm MS} = 0.81$, i.e., the MS companion is 81 per cent through its core hydrogen burning phase by time. Once the MS companion overflows its Roche lobe, the mass transfer phase could brighten Cygnus X-1 up to close to its Eddington luminosity of a few $\times 10^{39}$ erg s^{-1}. Once the envelope is removed, the companion will appear as a Wolf-Rayet (WR) star in an HMXB in a phase lasting for $\sim 3 \times 10^5$ years. In the default model described below, we apply WR mass loss with $f_{\rm WR} = 1$ to such a star.

[1] In Miller-Jones et al. (2021) the Roche-lobe filling factor is defined as the ratio between the distance from the center of the star to the point where the equipotential surface enclosing the volume of the star crosses the axis connecting the star to its BH companion, and the distance from the center of the star to the L1 Lagrange point. In this paper, we define the Roche-lobe filling factor as the ratio between the radius of the star and the volume-equivalent Roche-Lobe radius of Eggleton (1983). We therefore convert the median and one-σ lower bounds of 0.96 and 0.93 reported in table 1 of Miller-Jones et al. (2021) to values of 0.997 and 0.99, respectively, that we use here.

If we follow a treatment similar to Belczynski et al. (2011), in which the He core mass is determined by the mass of the star at the end of MS (after stripping in this case), we find the companion will collapse into a neutron star. Even if the binary survives the neutron star natal kick, which happens in 7% of all binaries in our models, it will generally be too wide to merge through gravitational-wave emission, with only a 0.12% probability that it will merge in 14 Gyr, similar to the findings of Belczynski et al. (2011). During this time, it may be detectable in radio pulsar surveys as a neutron-star – black-hole binary, although the non-recycled pulsar will likely only be observable as a radio source for a few tens of Myr. However, this treatment may significantly under-predict the core masses of stars that donated mass on the MS.

In our revised model, we address the potentially underestimated core mass of stripped MS donors under the assumption that this core mass is determined only by the mass of the star at the end of the MS. We account for the substantial amount of helium synthesized by the companion before interaction with the following crude approximation. We consider a constant rate of helium production during the MS, so the mass of helium produced is $M_{\rm He,MS} = \tau_{\rm MS} M_{\rm c,final}$, where $M_{\rm c,final}$ is the final helium core mass that would be achieved at the end of the MS phase for the given stellar mass, in the absence of mass transfer. Keeping track of the helium mass synthesized before stripping, $M_{\rm He,MS}$, leads to higher core masses at the end of the MS phase.

With this correction, we predict that in the absence of BH natal kicks, Cygnus X-1 will become a bound binary BH, but one that is too wide to merge within 14 Gyr. If we incorporate the COMPAS prescription for BH kicks based on the "delayed" model of Fryer et al. (2012), this changes to a 38% probability of surviving the kick and forming a bound binary BH, with a 4% probability that this binary will merge within 14 Gyr through gravitational-wave emission due to a fortuitous kick. However, the kick prescription for low-mass black holes that do not undergo complete fallback (Fryer et al. 2012) is rather uncertain, with conflicting evidence on the natal kick magnitudes of low-mass BHs (Repetto et al. 2017; Mandel 2016; Mirabel 2017; Wyrzykowski & Mandel 2020; Atri et al. 2019).

We also consider the impact of varying WR mass loss. Motivated by the results reported in figure 3 for $Z = 0.02$, we reduce $f_{\rm WR}$ to 0.2 from the value of 1 considered above. This increases the remnant mass of the current optical companion from $\sim 2.9 M_\odot$ to $\sim 5.7 M_\odot$, and the binary's probability of remaining bound after the supernova from 38% to 62%. With our adjusted prescription for the helium core mass of the stripped companion and $f_{\rm WR} = 0.2$, Cygnus X-1 has a 5% probability to merge within 14 Gyr as a binary BH.

We thus find that it is possible that a small fraction of HMXBs like Cygnus X-1 could form merging binary BHs, although this conclusion is sensitive to the treatment of mass transfer from MS donors in population synthesis models and to the natal kick distribution of relatively low-mass BHs. If systems like Cygnus X-1 do become progenitors of gravitational-wave events, this would impact the predicted spin distribution of merging binary black holes (Kushnir et al. 2016; Zaldarriaga et al. 2018; Belczynski et al. 2017; Fuller & Ma 2019; Bavera et al. 2020). Gravitational-wave observations could ultimately address this possibility by resolving the spin distribution with more events (e.g., Farr et al. 2017). Meanwhile, wide, non-merging binary BHs could potentially be observable through microlensing (Eilbott et al. 2017).

5. CYGNUS X-1: CAVEATS AND CONUNDRUMS

We show that the current properties of the Cygnus X-1 system imply a reduction in Wolf-Rayet wind mass loss rates for exposed HeMS stars. These results depend on several key assumptions.

We assumed that the optical companion did not experience Roche lobe overflow in its past. This assumption is consistent with the challenge of detaching from mass transfer once it commences given that the companion has roughly twice the mass of the BH, as explained in section 2.4. However, it is somewhat surprising that several HMXBs with well measured properties – Cygnus X-1, LMC X-1 and M33 X-7 – share not only a high BH spin, but also a similar evolutionary state. Selection effects favour observing bright, long-lived systems, i.e., those with massive main-sequence donors that are close to Roche lobe filling (enabling more efficient accretion). There may also be an evolutionary stalling point, increasing the number of systems in this phase.

The latter scenario could indicate that the systems do manage to detach and resume mass transfer multiple times. While this would negate our wind mass loss rate conclusions, it would imply that much less angular momentum is carried away during non-conservative mass transfer onto a BH than we expected. Assuming non-conservative mass transfer (valid if accretion onto a BH is Eddington-limited) from a donor that is twice as massive as the accretor, the specific angular momentum of the material ejected from the binary in units of the binary's specific orbital angular momentum must be $\gamma < 0.85$ in order to avoid a decrease in the size of the Roche lobe (see Eq. 2.1 for the change in orbital separation). For comparison, isotropic re-emission from the BH corresponds to $\gamma = 2$. Conversely, if $\gamma = 2$, the companion could still disengage from mass transfer if its radius shrinks faster than the size of the Roche lobe in response to mass loss. This would require the adiabatic logarithmic derivative of radius with respect to mass to exceed $\zeta \equiv d \log R / d \log M > 1.54$, which may be possible for stars in the late phase of their MS evolution that have already lost some mass.

It is also possible that the primary is not fully stripped during the mass transfer episode, but retains about $\sim 0.1\ M_{\odot}$ of its hydrogen envelope (e.g. Yoon et al. 2010; Yoon 2017; Bersten et al. 2014; Götberg et al. 2017, 2018; Laplace et al. 2020). The changed surface abundance could lead to reduced mass-loss rates until the remaining hydrogen is completely removed. However, it is not clear whether retaining an envelope of a fraction of a solar mass could be sufficient to prevent Wolf-Rayet-like winds. In any case, whether Wolf-Rayet wind mass loss rates must be lower than anticipated or whether stars that experience mass transfer in binaries are only partially stripped, the impact on binary evolution is similar: there is less mass loss than previously assumed. In fact, our Wolf-Rayet wind reduction factors can be broadly interpreted as constraints on winds from stripped stars, whether they are naked helium stars or retain a small hydrogen-rich envelope.

Naked helium cores can expand significantly in the last stages of their lives, potentially leading to another mass transfer episode from the BH progenitor late in the evolution. However, the degree of expansion is very mild for stars with initial masses $\gtrsim 20 M_{\odot}$ at near-solar metallicities (Yoon et al. 2010; Hirai 2017; Laplace et al. 2020), so Cygnus X-1 is unlikely to have experienced such mass transfer.

As a consequence of its mass accretion history, the secondary may be over-luminous relative to single stars of the same total mass (Dray & Tout 2007, but see Hellings 1983, who concludes that they MS accretors quickly return to single-star models, and Braun & Langer 1995, who reach the opposite conclusion and find that accretors are underluminous). Since we use single star evolutionary tracks to estimate the properties of the secondary star, this can affect our wind constraint from the no-RLOF condition. However, since we choose a stellar model that matches the observed radius of the secondary at the present day, we do not anticipate the impact to be significant.

Finally, as figure 3 shows, the level of reduction in the winds is sensitive to the assumed metallicity of Cygnus X-1. We now discuss this in more detail.

Shimanskii et al. (2012) report that helium, carbon, oxygen, aluminium, sulfur and iron are overabundant by [X/H]= 0.23–0.43 dex compared to the solar values (Anders & Grevesse 1989). Nitrogen, neon, and silicon have an even higher overabundance of [X/H]=0.69–0.94 dex. These values appear robust against variations due to orbital motion and Roche-lobe filling factors, although some hydrogen and helium lines are sensitive to variations in the wind (Shimanskii et al. 2012).

Previous accretion from the BH progenitor could significantly alter the chemical profile on the surface of the companion. For example, the detailed models of Qin et al. (2019) predict the observed enhancement of companion nitrogen abundances as a consequence of late main sequence mass transfer from the BH progenitor. In addition to direct accretion, which is expected to enhance helium and nitrogen abundances, the deposited angular momentum can lead to a dramatic spin-up of the MS star (e.g. Packet 1981), although spin-up to near break-up frequencies may suppress subsequent accretion. The surface could then be enhanced by helium and CNO-elements due to rotational mixing (Meynet & Maeder 2000; Heger & Langer 2000; Przybilla et al. 2010). The rotational mixing might also make the star overluminous compared to a non-rotating model (Langer 1992). The optical companion is observed to be tidally locked at present, with an inferred ratio of the rotational to orbital frequency of 1.05 ± 0.10 Miller-Jones et al. (2021). Assuming a present-day rotational period of 5.6 days, the rotational frequency is a third of the Keplerian (break-up) frequency at the stellar equator). Alternatively, as discussed above and contrary to the channel assumed in this work, the MS companion may have been partially stripped by mass transfer onto the BH or its progenitor after the initial mass transfer phase from the primary, revealing deeper layers of the star.

Although these mechanisms could be responsible for the overabundance of some of the elements, they have difficulty in explaining the overabundance of late stage burning elements such as silicon and iron. This implies that these elements were primordially enhanced or were deposited from the progenitor of the BH in the final stages of its evolution.

High primordial abundances imply that both stars in the binary had a high metallicity at birth, which therefore requires a very strong reduction in the mass-loss rate (a factor of ~ 10) following the constraints described in section 3. On the other hand, a weak explosion induced by the collapse of the core can lead to an ejection of a small fraction of the outer part of the envelope at very low velocities. Because most of the envelope is assumed to fall back into the BH, the ejected material will be barely above the escape velocity, and could be efficiently accreted by the companion in a RLOF-like manner. If the heavy elements synthesized at the centre are efficiently mixed up to the outer regions before the inner slower material starts falling back, these elements can accrete onto the surface of the secondary. Such efficient mixing of heavy elements has been observed in supernovae such as SN1987A and Cassiopeia A (e.g. Utrobin et al. 1995; Fesen et al. 2006), and has been reproduced in 3D supernova explosion simulations (e.g. Hammer et al. 2010; Wongwathanarat et al. 2015, 2017), while Liu et al. (2015); Hirai et al. (2018) explore the contamination of a MS companion by supernova ejecta. However, it is not clear whether similar degrees of mixing can be induced in failed supernovae that form BHs rather than neutron stars, and the abundance pattern of the Cygnus X-1 companion merits further investigation.

Regardless of whether we assume that the observed companion metallicity of $Z = 0.03$ (Shimanskii et al. 2012) is primordial, or use the lower metallicity of $Z = 0.01$ based on HD 227460 (Daflon et al. 2001), we conclude that the observed properties of Cygnus X-1 require a reduction in Wolf-Rayet winds to $\sim$ 5–40% of their previously assumed values in the context of our assumed evolutionary channel.

Recent theoretical modelling of mass-loss from stripped stars (Vink 2017; Sander et al. 2020; Sander & Vink 2020) points to reduced mass-loss rates compared to earlier literature. Moreover, these models suggest a steep dependence on the Eddington factor, which can change significantly during the lifetime of the stripped star. This indicates that extrapolating the empirical Wolf-Rayet mass-loss rates to the entire duration of the stripped star life is misleading. Our results are qualitatively consistent with these findings. The reduced mass-loss rates could also be attributed to strong wind clumping, which is expected to occur in line-driven winds due to radiative instabilities (Owocki et al. 1988; Sundqvist et al. 2018). Clumping of winds has been indirectly observed for massive MS stars in X-ray binaries (El Mellah et al. 2018; Lomaeva et al. 2020) and stripped stars may also experience high degrees of clumping.

We further find that HMXBs like Cygnus X-1 form through a different evolutionary channel than the bulk of merging binary black holes (see, e.g., Mandel & Farmer 2018, for a review). However, a fortuitous natal kick accompanying the birth of the secondary BH could lead Cygnus X-1 to merge as a BH binary within 14 Gyr. Gravitational-wave observations may be able to constrain the contribution of this channel to the formation of merging binary BHs through spin measurements.

ACKNOWLEDGEMENTS

Simulations in this paper made use of the COMPAS rapid binary population synthesis code, which is freely available at http://github.com/TeamCOMPAS/COMPAS. We thank Alexander Heger, Hagai Perets, Jerry Orosz, Stephen Justham, Selma de Mink and Jakub Klencki for discussions, and Robert Izzard and Silvia Toonen for comments on a preliminary draft of the manuscript. C. J. N. thanks the University of Birmingham for financial support. JCAM-J and IM are recipients of Australian Research Council Future Fellowships (FT140101082 and FT190100574, respectively). AVG acknowledges funding support by the Danish National Research Foundation (DNRF132).

REFERENCES

Adams, S. M., Kochanek, C. S., Gerke, J. R., Stanek, K. Z., & Dai, X. 2017, MNRAS, 468, 4968, doi: 10.1093/mnras/stx816

Anders, E., & Grevesse, N. 1989, GeoCoA, 53, 197, doi: 10.1016/0016-7037(89)90286-X

Asplund, M., Grevesse, N., Sauval, A. J., & Scott, P. 2009, ARA&A, 47, 481, doi: 10.1146/annurev.astro.46.060407.145222

Atri, P., Miller-Jones, J. C. A., Bahramian, A., et al. 2019, MNRAS, 489, 3116, doi: 10.1093/mnras/stz2335

Axelsson, M., Church, R. P., Davies, M. B., Levan, A. J., & Ryde, F. 2011, MNRAS, 412, 2260, doi: 10.1111/j.1365-2966.2010.18050.x

Bardeen, J. M., Carter, B., & Hawking, S. W. 1973, Communications in Mathematical Physics, 31, 161, doi: 10.1007/BF01645742

Barrett, J. W., Gaebel, S. M., Neijssel, C. J., et al. 2018, MNRAS, 477, 4685, doi: 10.1093/mnras/sty908

Batta, A., & Ramirez-Ruiz, E. 2019, arXiv e-prints, arXiv:1904.04835. https://arxiv.org/abs/1904.04835

Batta, A., Ramirez-Ruiz, E., & Fryer, C. 2017, ApJL, 846, L15, doi: 10.3847/2041-8213/aa8506

Bavera, S. S., Fragos, T., Qin, Y., et al. 2020, A&A, 635, A97, doi: 10.1051/0004-6361/201936204

Belczynski, K., Bulik, T., & Bailyn, C. 2011, ApJL, 742, L2, doi: 10.1088/2041-8205/742/1/L2

Belczynski, K., Bulik, T., Fryer, C. L., et al. 2010, ApJ, 714, 1217, doi: 10.1088/0004-637X/714/2/1217

Belczynski, K., Klencki, J., Fields, C. E., et al. 2017, arXiv e-prints, arXiv:1706.07053. https://arxiv.org/abs/1706.07053

Bersten, M. C., Benvenuto, O. G., Folatelli, G., et al. 2014, AJ, 148, 68, doi: 10.1088/0004-6256/148/4/68

Bisiacchi, G. F., Dultzin, D., Firmani, C., & Hacyan, S. 1974, ApJL, 190, L59, doi: 10.1086/181504

Blaauw, A. 1961, BAN, 15, 265

Bolton, C. T. 1972, Nature, 235, 271, doi: 10.1038/235271b0

—. 1975, ApJ, 200, 269, doi: 10.1086/153785

Bouret, J. C., Hillier, D. J., Lanz, T., & Fullerton, A. W. 2012, A&A, 544, A67, doi: 10.1051/0004-6361/201118594

Braun, H., & Langer, N. 1995, A&A, 297, 483

Brott, I., de Mink, S. E., Cantiello, M., et al. 2011, A&A, 530, A115, doi: 10.1051/0004-6361/201016113

Cantiello, M., Mankovich, C., Bildsten, L., Christensen-Dalsgaard, J., & Paxton, B. 2014, ApJ, 788, 93, doi: 10.1088/0004-637X/788/1/93

Conti, P. S. 1975, Memoires of the Societe Royale des Sciences de Liege, 9, 193

—. 1978, A&A, 63, 225

Daflon, S., Cunha, K., Becker, S. R., & Smith, V. V. 2001, ApJ, 552, 309, doi: 10.1086/320460

Davidson, K., & Ostriker, J. P. 1973, ApJ, 179, 585, doi: 10.1086/151897

de Mink, S. E., Langer, N., Izzard, R. G., Sana, H., & de Koter, A. 2013, ApJ, 764, 166, doi: 10.1088/0004-637X/764/2/166

Dray, L. M., & Tout, C. A. 2007, MNRAS, 376, 61, doi: 10.1111/j.1365-2966.2007.11431.x

Eggleton, P. P. 1983, ApJ, 268, 368, doi: 10.1086/160960

Eilbott, D. H., Riley, A. H., Cohn, J. H., Kesden, M., & King, L. J. 2017, MNRAS, 467, L100, doi: 10.1093/mnrasl/slx007

El Mellah, I., Sundqvist, J. O., & Keppens, R. 2018, MNRAS, 475, 3240, doi: 10.1093/mnras/stx3211

Eldridge, J. J., Stanway, E. R., Xiao, L., et al. 2017, PASA, 34, e058, doi: 10.1017/pasa.2017.51

Fabian, A. C., Wilkins, D. R., Miller, J. M., et al. 2012, MNRAS, 424, 217, doi: 10.1111/j.1365-2966.2012.21185.x

Farr, W. M., & Mandel, I. 2018, Science, 361, aat6506, doi: 10.1126/science.aat6506

Farr, W. M., Stevenson, S., Miller, M. C., et al. 2017, Nature, 548, 426, doi: 10.1038/nature23453

Fernández, R., Quataert, E., Kashiyama, K., & Coughlin, E. R. 2018, MNRAS, 476, 2366, doi: 10.1093/mnras/sty306

Fesen, R. A., Hammell, M. C., Morse, J., et al. 2006, ApJ, 636, 859, doi: 10.1086/498092

Fragos, T., & McClintock, J. E. 2015, ApJ, 800, 17, doi: 10.1088/0004-637X/800/1/17

Fryer, C. L. 2004, ApJL, 601, L175, doi: 10.1086/382044

Fryer, C. L., Belczynski, K., Wiktorowicz, G., et al. 2012, ApJ, 749, 91, doi: 10.1088/0004-637X/749/1/91

Fukuda, I. 1982, PASP, 94, 271, doi: 10.1086/130977

Fuller, J., & Ma, L. 2019, ApJL, 881, L1, doi: 10.3847/2041-8213/ab339b

Fuller, J., Piro, A. L., & Jermyn, A. S. 2019, MNRAS, 485, 3661, doi: 10.1093/mnras/stz514

Götberg, Y., de Mink, S. E., & Groh, J. H. 2017, A&A, 608, A11, doi: 10.1051/0004-6361/201730472

Götberg, Y., de Mink, S. E., Groh, J. H., et al. 2018, A&A, 615, A78, doi: 10.1051/0004-6361/201732274

Gou, L., McClintock, J. E., Reid, M. J., et al. 2011, ApJ, 742, 85, doi: 10.1088/0004-637X/742/2/85

Gräfener, G., & Hamann, W. R. 2005, A&A, 432, 633, doi: 10.1051/0004-6361:20041732

Grinberg, V., Hell, N., El Mellah, I., et al. 2017, A&A, 608, A143, doi: 10.1051/0004-6361/201731843

Hamann, W. R., & Koesterke, L. 1998, A&A, 335, 1003

Hamann, W. R., Koesterke, L., & Wessolowski, U. 1995, A&A, 299, 151

Hammer, N. J., Janka, H. T., & Müller, E. 2010, ApJ, 714, 1371, doi: 10.1088/0004-637X/714/2/1371

Heger, A., & Langer, N. 2000, ApJ, 544, 1016, doi: 10.1086/317239

Hellings, P. 1983, Ap&SS, 96, 37, doi: 10.1007/BF00661941

Hirai, R. 2017, MNRAS, 466, 3775, doi: 10.1093/mnras/stw3321

Hirai, R., Podsiadlowski, P., & Yamada, S. 2018, ApJ, 864, 119, doi: 10.3847/1538-4357/aad6a0

Hirschi, R., Meynet, G., & Maeder, A. 2005, A&A, 443, 581, doi: 10.1051/0004-6361:20053329

Humphreys, R. M., & Davidson, K. 1994, PASP, 106, 1025, doi: 10.1086/133478

Hurley, J. R., Pols, O. R., & Tout, C. A. 2000, MNRAS, 315, 543, doi: 10.1046/j.1365-8711.2000.03426.x

Hurley, J. R., Tout, C. A., & Pols, O. R. 2002, MNRAS, 329, 897, doi: 10.1046/j.1365-8711.2002.05038.x

Hutchings, J. B., Crampton, D., Glaspey, J., & Walker, G. A. H. 1973, ApJ, 182, 549, doi: 10.1086/152163

Ingram, A., van der Klis, M., Middleton, M., et al. 2016, MNRAS, 461, 1967, doi: 10.1093/mnras/stw1245

Izzard, R. G., Ramirez-Ruiz, E., & Tout, C. A. 2004, MNRAS, 348, 1215, doi: 10.1111/j.1365-2966.2004.07436.x

Janka, H.-T. 2013, MNRAS, 434, 1355, doi: 10.1093/mnras/stt1106

—. 2017, ApJ, 837, 84, doi: 10.3847/1538-4357/aa618e

Kawano, T., Done, C., Yamada, S., et al. 2017, PASJ, 69, 36, doi: 10.1093/pasj/psx009

King, A. R., & Kolb, U. 1999, MNRAS, 305, 654, doi: 10.1046/j.1365-8711.1999.02482.x

Kippenhahn, R., Ruschenplatt, G., & Thomas, H. C. 1980, A&A, 91, 175

Kippenhahn, R., Weigert, A., & Weiss, A. 2012, Stellar Structure and Evolution, doi: 10.1007/978-3-642-30304-3

Köhler, K., Langer, N., de Koter, A., et al. 2015, A&A, 573, A71, doi: 10.1051/0004-6361/201424356

Kushnir, D., Zaldarriaga, M., Kollmeier, J. A., & Waldman, R. 2016, MNRAS, 462, 844, doi: 10.1093/mnras/stw1684

Langer, N. 1992, A&A, 265, L17

Langer, N., Cantiello, M., Yoon, S.-C., et al. 2008, in IAU Symposium, Vol. 250, Massive Stars as Cosmic Engines, ed. F. Bresolin, P. A. Crowther, & J. Puls, 167–178, doi: 10.1017/S1743921308020462

Laplace, E., Götberg, Y., de Mink, S. E., Justham, S., & Farmer, R. 2020, A&A, 637, A6, doi: 10.1051/0004-6361/201937300

Liu, Z.-W., Tauris, T. M., Röpke, F. K., et al. 2015, A&A, 584, A11, doi: 10.1051/0004-6361/201526757

Lomaeva, M., Grinberg, V., Guainazzi, M., et al. 2020, A&A, 641, A144, doi: 10.1051/0004-6361/202037807

Lovegrove, E., & Woosley, S. E. 2013, ApJ, 769, 109, doi: 10.1088/0004-637X/769/2/109

MacLeod, M., & Loeb, A. 2020, arXiv e-prints, arXiv:2007.07252. https://arxiv.org/abs/2007.07252
Maeder, A., Georgy, C., & Meynet, G. 2008, A&A, 479, L37, doi: 10.1051/0004-6361:20079007
Mahy, L., Rauw, G., De Becker, M., Eenens, P., & Flores, C. A. 2015, A&A, 577, A23, doi: 10.1051/0004-6361/201321985
Mandel, I. 2016, MNRAS, 456, 578, doi: 10.1093/mnras/stv2733
Mandel, I., & de Mink, S. E. 2016, MNRAS, 458, 2634, doi: 10.1093/mnras/stw379
Mandel, I., & Farmer, A. 2018, ArXiv e-prints. https://arxiv.org/abs/1806.05820
Mandel, I., & Fragos, T. 2020, arXiv e-prints, arXiv:2004.09288. https://arxiv.org/abs/2004.09288
Marchant, P., Langer, N., Podsiadlowski, P., Tauris, T. M., & Moriya, T. J. 2016, A&A, 588, A50, doi: 10.1051/0004-6361/201628133
Marti, J., Rodriguez, L. F., Mirabel, I. F., & Paredes, J. M. 1996, A&A, 306, 449
Meynet, G., & Maeder, A. 2000, A&A, 361, 101. https://arxiv.org/abs/astro-ph/0006404
Miller, M. C., & Miller, J. M. 2015, PhR, 548, 1, doi: 10.1016/j.physrep.2014.09.003
Miller-Jones, J., et al. 2021, Cygnus X-1 contains a 21-solar mass black hole - Implications for massive star winds, doi: 10.1126/science.abb3363
Mirabel, F. 2017, New Astronomy Reviews, 78, 1, doi: 10.1016/j.newar.2017.04.002
Mirabel, I. F., & Rodrigues, I. 2003, Science, 300, 1119, doi: 10.1126/science.1083451
Moffat, A. F. J., Drissen, L., Lamontagne, R., & Robert, C. 1988, ApJ, 334, 1038, doi: 10.1086/166895
Murguia-Berthier, A., Batta, A., Janiuk, A., et al. 2020, arXiv e-prints, arXiv:2005.10212. https://arxiv.org/abs/2005.10212
Nadezhin, D. K. 1980, Ap&SS, 69, 115, doi: 10.1007/BF00638971
Neijssel, C. J., Vigna-Gómez, A., Stevenson, S., et al. 2019, MNRAS, 490, 3740, doi: 10.1093/mnras/stz2840
Nelemans, G., Tauris, T. M., & van den Heuvel, E. P. J. 1999, A&A, 352, L87. https://arxiv.org/abs/astro-ph/9911054
Nugis, T., Crowther, P. A., & Willis, A. J. 1998, A&A, 333, 956
Nugis, T., & Lamers, H. J. G. L. M. 2000, A&A, 360, 227
Orosz, J. A., McClintock, J. E., Aufdenberg, J. P., et al. 2011, ApJ, 742, 84, doi: 10.1088/0004-637X/742/2/84
Owocki, S. P., Castor, J. I., & Rybicki, G. B. 1988, ApJ, 335, 914, doi: 10.1086/166977
Packet, W. 1981, A&A, 102, 17
Paxton, B., Bildsten, L., Dotter, A., et al. 2011, ApJS, 192, 3, doi: 10.1088/0067-0049/192/1/3
Petrovic, J., Langer, N., Yoon, S. C., & Heger, A. 2005, A&A, 435, 247, doi: 10.1051/0004-6361:20042545
Petterson, J. A. 1978, ApJ, 224, 625, doi: 10.1086/156411
Podsiadlowski, P., Rappaport, S., & Han, Z. 2003, MNRAS, 341, 385, doi: 10.1046/j.1365-8711.2003.06464.x
Pols, O. R., Schröder, K.-P., Hurley, J. R., Tout, C. A., & Eggleton, P. P. 1998, MNRAS, 298, 525, doi: 10.1046/j.1365-8711.1998.01658.x
Przybilla, N., Firnstein, M., Nieva, M. F., Meynet, G., & Maeder, A. 2010, A&A, 517, A38, doi: 10.1051/0004-6361/201014164
Qin, Y., Marchant, P., Fragos, T., Meynet, G., & Kalogera, V. 2019, ApJL, 870, L18, doi: 10.3847/2041-8213/aaf97b
Ramírez-Agudelo, O. H., Simón-Díaz, S., Sana, H., et al. 2013, A&A, 560, A29, doi: 10.1051/0004-6361/201321986
Ramírez-Agudelo, O. H., Sana, H., de Mink, S. E., et al. 2015, A&A, 580, A92, doi: 10.1051/0004-6361/201425424
Rao, A., Gandhi, P., Knigge, C., et al. 2019, arXiv e-prints, arXiv:1908.00810. https://arxiv.org/abs/1908.00810
Renzo, M., Ott, C. D., Shore, S. N., & de Mink, S. E. 2017, A&A, 603, A118, doi: 10.1051/0004-6361/201730698
Repetto, S., Igoshev, A. P., & Nelemans, G. 2017, MNRAS, 467, 298, doi: 10.1093/mnras/stx027
Rosen, A. L., Krumholz, M. R., & Ramirez-Ruiz, E. 2012, ApJ, 748, 97, doi: 10.1088/0004-637X/748/2/97
Russell, D. M., Fender, R. P., Gallo, E., & Kaiser, C. R. 2007, MNRAS, 376, 1341, doi: 10.1111/j.1365-2966.2007.11539.x
Sander, A. A. C., Hamann, W. R., Todt, H., Hainich, R., & Shenar, T. 2017, A&A, 603, A86, doi: 10.1051/0004-6361/201730642
Sander, A. A. C., & Vink, J. S. 2020, MNRAS, 499, 873, doi: 10.1093/mnras/staa2712
Sander, A. A. C., Vink, J. S., & Hamann, W. R. 2020, MNRAS, 491, 4406, doi: 10.1093/mnras/stz3064
Schrøder, S. L., Batta, A., & Ramirez-Ruiz, E. 2018, ApJL, 862, L3, doi: 10.3847/2041-8213/aacf8d
Sell, P. H., Heinz, S., Richards, E., et al. 2015, MNRAS, 446, 3579, doi: 10.1093/mnras/stu2320
Shimanskii, V. V., Karitskaya, E. A., Bochkarev, N. G., et al. 2012, Astronomy Reports, 56, 741, doi: 10.1134/S106377291210006X
Spruit, H. C. 2002, A&A, 381, 923, doi: 10.1051/0004-6361:20011465
Stella, L., & Vietri, M. 1998, ApJL, 492, L59, doi: 10.1086/311075
Stevenson, S., Vigna-Gómez, A., Mandel, I., et al. 2017, Nature Communications, 8, 14906, doi: 10.1038/ncomms14906
Stirling, A. M., Spencer, R. E., de la Force, C. J., et al. 2001, MNRAS, 327, 1273, doi: 10.1046/j.1365-8711.2001.04821.x
Sundqvist, J. O., Owocki, S. P., & Puls, J. 2018, A&A, 611, A17, doi: 10.1051/0004-6361/201731718
Takahashi, K., & Langer, N. 2020, arXiv e-prints, arXiv:2010.13909. https://arxiv.org/abs/2010.13909
Tayler, R. J. 1973, MNRAS, 161, 365, doi: 10.1093/mnras/161.4.365
Thorne, K. S. 1974, ApJ, 191, 507, doi: 10.1086/152991

Utrobin, V. P., Chugai, N. N., & Andronova, A. A. 1995, A&A, 295, 129

Valsecchi, F., Glebbeek, E., Farr, W. M., et al. 2010, Nature, 468, 77, doi: 10.1038/nature09463

van den Heuvel, E. P. J. 1975, ApJL, 198, L109, doi: 10.1086/181824

van Son, L. A. C., De Mink, S. E., Broekgaarden, F. S., et al. 2020, ApJ, 897, 100, doi: 10.3847/1538-4357/ab9809

Vigna-Gómez, A., Neijssel, C. J., Stevenson, S., et al. 2018, MNRAS, 481, 4009, doi: 10.1093/mnras/sty2463

Vink, J. S. 2017, A&A, 607, L8, doi: 10.1051/0004-6361/201731902

Vink, J. S., & de Koter, A. 2005, A&A, 442, 587, doi: 10.1051/0004-6361:20052862

Vink, J. S., de Koter, A., & Lamers, H. J. G. L. M. 2001, A&A, 369, 574, doi: 10.1051/0004-6361:20010127

Webster, B. L., & Murdin, P. 1972, Nature, 235, 37, doi: 10.1038/235037a0

Wong, T.-W., Valsecchi, F., Fragos, T., & Kalogera, V. 2012, ApJ, 747, 111, doi: 10.1088/0004-637X/747/2/111

Wongwathanarat, A., Janka, H.-T., Müller, E., Pllumbi, E., & Wanajo, S. 2017, ApJ, 842, 13, doi: 10.3847/1538-4357/aa72de

Wongwathanarat, A., Müller, E., & Janka, H. T. 2015, A&A, 577, A48, doi: 10.1051/0004-6361/201425025

Wyrzykowski, Ł., & Mandel, I. 2020, A&A, 636, A20, doi: 10.1051/0004-6361/201935842

Yoon, S.-C. 2017, MNRAS, 470, 3970, doi: 10.1093/mnras/stx1496

Yoon, S. C., Woosley, S. E., & Langer, N. 2010, ApJ, 725, 940, doi: 10.1088/0004-637X/725/1/940

Zahn, J.-P. 1977, A&A, 57, 383

Zaldarriaga, M., Kushnir, D., & Kollmeier, J. A. 2018, MNRAS, 473, 4174, doi: 10.1093/mnras/stx2577

Zhao, X., et al. 2021, Reestimating the Spin Parameter of the Black Hole in Cygnus X-1

APPENDIX

A. WIND MASS-LOSS RATE FOR STRIPPED STARS

In this appendix, we describe the particular parametrized formalism we used to model wind-driven mass loss from stripped stars. While more recent theoretical models are available (e.g., Vink 2017; Sander et al. 2020), this provides us with a convenient framework for investigating the empirical constraints placed by Cygnus X-1.

Hamann et al. (1995) formulated a prescription for the wind mass loss rate for stripped or Wolf-Rayet stars as a function of the mass and luminosity of the stripped star. Hamann & Koesterke (1998) expanded on this work by reducing winds by a factor of $\sqrt{D}$ where D is the wind clumping factor (Moffat et al. 1988; Nugis et al. 1998). Vink & de Koter (2005) further introduced a metallicity dependence to the winds. Combining the effects of clumping and metallicity leads to the prescription

$$(dM/dt)_{\rm WR} = \underbrace{\frac{1}{\sqrt{D}} 10^{-11.95} \frac{L}{L_\odot}^{1.5}}_{1} \underbrace{\frac{Z}{Z_\odot}^{0.86}}_{2} \ {\rm M_\odot \ yr^{-1}}, \tag{A1}$$

where term 1 is the result of Hamann et al. (1995); Hamann & Koesterke (1998) and term 2 is from Vink & de Koter (2005). Setting $D = 100$, i.e., reducing winds by a factor of 10, recovers Eq.(9) of Belczynski et al. (2010) and is consistent with the winds of Yoon et al. (2010).

We follow Barrett et al. (2018) in scaling the prescription of Belczynski et al. (2010) by a multiplicative factor $f_{\rm WR}$ in order to parametrise the uncertainty in the wind mass-loss rates:

$$(dM/dt)_{\rm WR} = f_{\rm WR} \times 10^{-13} \frac{L}{L_\odot}^{1.5} \frac{Z}{Z_\odot}^{0.86} \ {\rm M_\odot \ yr^{-1}}. \tag{A2}$$

Note that this is not the same $f_{\rm WR}$ as used in Yoon et al. (2010) because ours already assumes a reduction of the original wind prescription of Hamann et al. (1995). The default assumption of $f_{\rm WR} = 1$ corresponds to the default models of Belczynski et al. (2010); Yoon et al. (2010); Stevenson et al. (2017); Qin et al. (2019).

It is challenging to interpret our constraints on $f_{\rm WR}$ in terms of a wind clumping factor D. A direct interpretation of $f_{\rm WR} = 0.2$ would imply a clumping factor of $D = 2500$ in the model of Eq. (A1). Nugis et al. (1998); Nugis & Lamers (2000) used a clumping factor ranging from 10 to 30; D could be as high as 16 according to Hamann & Koesterke (1998). More recent theoretical models by Sander et al. (2017) use depth-dependent clumping factors and suggest a maximum value at infinity of $D_\infty = 10$ to be consistent with observations of electron scattering wings. In later works however, Sander et al. (2020) and Sander & Vink (2020) propose 50 as a maximum upper limit for D_∞, by comparison with previous theoretical works (Gräfener & Hamann 2005) and O/B star analyses (e.g. Bouret et al. 2012; Mahy et al. 2015). A clumping factor of 2500 seems extraordinary compared to previous models. As mentioned in the Section 5, additional constraints on the clumpiness of stellar winds from massive stars can be obtained from X-ray binaries (e.g. Lomaeva et al. 2020; El Mellah et al. 2018; Grinberg et al. 2017).

In light of the above, our reduction of $f_{\rm WR}$ is probably best interpreted as an overall constraint on mass loss from massive stripped stars (Vink 2017), perhaps indicating a different dependence on metallicity or luminosity (cf. Sander et al. 2020; Sander & Vink 2020), rather than a specific change in the clumping.